

# ANALYSIS OF AN EXTENDED PMART FOR CT IMAGE RECONSTRUCTION AS A NONLINEAR DYNAMICAL SYSTEM

Tetsuya Yoshinaga

*The University of Tokushima*

*3-18-15 Kuramoto, Tokushima, 770-8509 Japan*

**Keywords:** CT, iterative image reconstruction, PMART, nonlinear dynamical system, bifurcation.

**Abstract:** Among iterative image reconstruction algorithms for computed tomography (CT), it is known that the power multiplicative algebraic reconstruction technique (PMART) has a good property for convergence speed and maximization of entropy. In this paper, we investigate an extended PMART, which is a dynamical class for accelerating the convergence. The convergence process of the state in the neighborhood of the true reconstructed image can be reduced to the property of a fixed point observed in the dynamical system. For investigating convergence speed, we present a computational method of obtaining parameter sets in which a given real or absolute value of the characteristic multiplier is equal. The advantage of the extended PMART is verified by comparing with the standard multiplicative algebraic reconstruction technique (MART) using numerical experiments.

## 1 INTRODUCTION

Iterative reconstruction technique (Gordon et al., 1970; Kak and Slaney, 1987; Stark, 1987; Shepp and Vardi, 1982) is known as a method to reconstruct images of computed tomography (CT), and has advantages for reducing artifacts against the filtered backprojection procedure, which is commonly used for CT reconstruction in practice. Because of the high-quality reconstructions, there has been a lot of research (Gordon and Herman, 1974; Snyder et al., 1992; Herman and Meyer, 1993; Wang et al., 1996; Mueller et al., 1999; Man et al., 2001; Byrne, 2004) improving the iterative deblurring procedures. Among the iterative reconstruction algorithms, the power multiplicative algebraic reconstruction technique (PMART) (Badea and Gordon, 2004; Byrne, 2004) has a good property for maximizing entropy, however, it requires a large number of iterations to obtain the final reconstruction image for large data sets. In order to improve the convergence speed, we propose an extended PMART, which is a dynamical class including the multiplicative algebraic reconstruction technique (MART) as well as the PMART. The convergence process of the state in the neighborhood of the true reconstructed image can be reduced to the property of a fixed point observed in the dynamical

system. For investigating convergence behavior, we present a computational method of obtaining parameter sets in which a given real or absolute value of the characteristic multiplier is equal. The advantage of the extended PMART is verified by comparing with the standard MART using numerical experiments.

## 2 METHOD OF ANALYSIS

Each iterative reconstruction procedure treated in this paper is considered as a nonlinear dynamical system. Theoretical background and methods for analysis using qualitative bifurcation theory are summarized in this section. The procedure of numerical calculation in Sect.2.2 is a novel method for the purpose of studying convergence process observed in the dynamical system.

### 2.1 Fixed Point and its Bifurcation

We consider a discrete dynamical system or a general map defined by

$$T_\nu : R^n \rightarrow R^n ; x^{(k)} \mapsto x^{(k+1)} = T_\nu(x^{(k)}) \quad (1)$$

where  $x \in R^n$  is the state of discrete time  $k = 1, 2, \dots$ , and  $\nu \in R$  is a system parameter. The point

$x^*$  satisfying

$$x^* - T_\nu^m(x^*) = 0 \quad (2)$$

becomes a fixed ( $m = 1$ ) or an  $m$ -periodic ( $m > 1$ ) point of  $T_\nu$ . Let  $x^*$  be a periodic point of  $T_\nu$ , then the characteristic equation of the periodic point  $x^*$  is defined by

$$\chi(x^*, \nu, \mu) = \det(\mu E - DT_\nu^m(x^*)) = 0 \quad (3)$$

where  $E$  is the  $n \times n$  identity matrix, and  $DT_\nu^m$  denotes the derivative of  $T_\nu^m$ . We call  $x^*$  is hyperbolic, if all the absolute values of the eigenvalues of  $T_\nu^m$  are different from unity. Note that an  $m$ -periodic point can be studied by replacing  $T_\nu$  with  $T_\nu^m$ ,  $m$ th iterates of  $T_\nu$ , in Eq.(2). Therefore in the following we consider only properties of a fixed point of  $T_\nu$ . Similar argument can be applied to the periodic point of  $T_\nu$ .

Now we consider a topological classification of hyperbolic fixed point. Let  $x^*$  be a hyperbolic fixed point and  $E^u$  be the intersection of  $R^n$  and the direct sum of the generalized eigenspaces of  $DT_\nu(x^*)$  corresponding to the eigenvalues  $\mu$  such that  $|\mu| > 1$ . Let  $L^u = DT_\nu(x^*)|_{E^u}$ . Then the topological type of a hyperbolic fixed point is determined by  $\dim E^u$  and the orientation preserving or reserving property of  $L^u$ .

We define four types of hyperbolic fixed points:

1. *PD*-type if  $\dim E^u$  is even and  $\det L^u > 0$ ,
2. *ND*-type if  $\dim E^u$  is odd and  $\det L^u > 0$ ,
3. *PI*-type if  $\dim E^u$  is even and  $\det L^u < 0$ , and
4. *NI*-type if  $\dim E^u$  is odd and  $\det L^u < 0$ .

From the definition, at a *PD*- or an *ND*-type of fixed point  $x^*$ ,  $L^u$  is an orientation preserving mapping, whereas at a *PI*- or an *NI*-type of fixed point  $x^*$ ,  $T_\nu$  is an orientation reversing mapping. If  $E^u$  is the empty set, we identify  $x^*$  as a *PD*-type. We use the symbol  ${}_\ell M^m$  for a hyperbolic periodic point, where  $M$  denotes one of the types *PD*, *ND*, *PI* and *NI*, and  $\ell$  indicates the number of characteristic multiplier outside the unit circle in the complex plane, and  $m$  indicates  $m$ -periodic point, which will be omitted for  $m = 1$ .

Bifurcation occurs when the topological type of a fixed point is changed by the variation of a system parameter. The generic codimension-one bifurcations are: tangent bifurcation, period-doubling bifurcation, and the Neimark-Sacker bifurcation. These bifurcations are observed when the hyperbolicity is destroyed, which corresponds to the critical distribution of the characteristic multiplier  $\mu$  such that  $\mu = +1$  for tangent bifurcation,  $\mu = -1$  for period-doubling bifurcation, and  $\mu = e^{j\theta}$  for the Neimark-Sacker bifurcation, where  $j = \sqrt{-1}$ .

## 2.2 Equal Characteristic Multiplier

The convergence behavior in the neighborhood of a stable fixed point is governed by characteristic multipliers or eigenvalues of the derivative of  $T_\nu$  with respect to the fixed point. To investigate parameter region in which the system has locally faster convergence speed, we propose a method for calculating a set of both parameter and fixed point with a given equal real or absolute value of the characteristic multiplier.

**In the case of real characteristic multiplier:** When the specified real characteristic multiplier is denoted by  $\mu^*$ , the condition is given by

$$\chi(x, \nu, \mu^*) = \det(\mu^* E - DT_\nu(x)) = 0 \quad (4)$$

Therefore we can obtain unknown set  $(x, \nu) \in R^n \times R$  by solving the fixed point equation of Eq.(2) and the condition of Eq.(4), simultaneously.

**In the case of complex characteristic multiplier:** When the specified absolute value of the characteristic multiplier is denoted by  $\rho^*$ , the condition is given by

$$\chi(x, \nu, \rho^* e^{j\theta}) = \det(\rho^* e^{j\theta} E - DT_\nu(x)) = 0 \quad (5)$$

where  $j$  is the imaginary unit, and  $\theta$  is the argument of a complex characteristic multiplier. For obtaining unknown set  $(x, \nu, \theta) \in R^n \times R \times R$ , we solve simultaneous equations consisting of the fixed point equation Eq.(2) and the following two equations:

$$\begin{aligned} \chi_1(x, \nu, \rho^* e^{j\theta}) &= \Re [\det(\rho^* e^{j\theta} E - DT_\nu(x))] = 0 \\ \chi_2(x, \nu, \rho^* e^{j\theta}) &= \Im [\det(\rho^* e^{j\theta} E - DT_\nu(x))] = 0 \end{aligned} \quad (6)$$

where  $\Re$  and  $\Im$  denote the real and the imaginary parts, respectively.

For the numerical determination of the above sets, Newton's method is used. The Jacobian matrix of the set of equations is derived from the first and the second derivatives of the map  $T_\nu$ . This procedure is an extension of Kawakami's method (Kawakami, 1984) for finding bifurcation parameters.

## 3 DYNAMICS OF AN EXTENDED PMART

Consider a  $J$ -dimensional discrete dynamical system  $x^{(k+1)} = f(x^{(k)})$ ,  $k = 1, 2, \dots$ , or a map defined by

$$f : R^J \rightarrow R^J ; x \mapsto f(x) \quad (7)$$

where  $x^{(k)}$  and  $x = (x_1, x_2, \dots, x_J)^T$  are state vectors in  $R^J$ , each of which corresponds to the successive estimate of the reconstructed value of an iterative algorithm in image reconstruction. The PMART can be written in the mapping form with the following elements  $f_j$ s for  $j = 1, 2, \dots, J$ :  $f_j = f_j^I \circ f_j^{I-1} \circ \dots \circ f_j^1$  with  $i$ th submap

$$f_j^i = x_j \left( \frac{q^i}{p^i x} \right)^{\gamma p_j^i} \quad (8)$$

where  $p^i = (p_1^i, p_2^i, \dots, p_J^i)$  is the normalized projection operator applied on the  $x$  image,  $q^i$  and  $p^i x$  are respectively the projection and the reprojection values, corresponding to the  $i$ th ray, for  $i = 1, 2, \dots, I$ , and  $\gamma$  is a positive real parameter.

The derivative of  $f$  with respect to  $x$  is given by  $\frac{\partial f}{\partial x} = \frac{\partial f^I}{\partial x} \frac{\partial f^{I-1}}{\partial x} \dots \frac{\partial f^1}{\partial x}$  and the derivative of each submap  $f^i$  can be obtained by

$$\frac{\partial f^i}{\partial x} = \text{diag}_j \left\{ \left( \frac{q^i}{p^i x} \right)^{\gamma p_j^i} \right\} \times \left( E - \frac{\gamma}{p^i x} \text{diag}_j \{x_j\} \cdot p^i \cdot p^{iT} \right)$$

for  $i = 1, 2, \dots, I$ , where  $E$  denotes the  $J \times J$  identity matrix. By direct calculation, we see that the eigenvalues of the Jacobian  $\partial f^i / \partial x$  at a fixed point of  $f$  are  $(1 - \gamma)$  and  $(J - 1)$  ones. Therefore when the value of  $\gamma$  is 2 or the critical power (Badea and Gordon, 2004), the absolute values of the determinants of the derivatives for the map  $f$  as well as each submap  $f^i$  at the fixed point are all 1, and every characteristic multiplier of the fixed point is located on the unit circle in the complex plane. Moreover the fixed point is stable and unstable when the values of  $\gamma$  are less and greater than 2, respectively.

We now consider a dynamical system defined by

$$g : R^J \rightarrow R^J ; x \mapsto (1 - \lambda)x + \lambda f(x) \quad (9)$$

where  $f$  denotes the map of the PMART in Eq.(7) with Eq.(8), and  $\lambda \in R$  is a parameter. Note that the expression Eq.(9) includes the algorithm of the MART (Badea and Gordon, 2004) when  $\lambda = 1$  and  $\gamma = 1$ .

As discussed above, in the case of  $J \geq 2$ , a higher codimension bifurcation satisfying multiple generic bifurcation conditions including the Neimark-Sacker bifurcation, of the nonhyperbolic fixed point occurs in the dynamical system  $f$  at  $\gamma = 2$ . Then an invariant closed curve (ICC) generates around the fixed point in the state space. When  $\gamma < 2$ , the ICC disappears and iterative points converge to the stable fixed point along the center manifold that is qualitatively equivalent to the spiral. Due to the attracting spiral behavior, it is expected that  $g(x)$ , which is considered

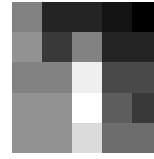


Figure 1: Phantom image of 5 × 5 pixels.

as a weighted average of the point  $x$  and the next iterate  $f(x)$ , obtains a better estimate than  $f(x)$  for an appropriate value of  $\lambda$ .

## 4 EXPERIMENTAL RESULTS AND DISCUSSION

To illustrate the efficiency of the proposed iterative algorithm and the computational method, we treat two examples: (i) the first image is made of four pixels and six projection rays with the projection operator  $p^1 = (1, 1, 0, 0)$ ,  $p^2 = (0, 0, 1, 1)$ ,  $p^3 = (1, 0, 0, 1)$ ,  $p^4 = (0, 1, 0, 1)$ ,  $p^5 = (1, 0, 1, 0)$ , and  $p^6 = (0, 1, 1, 0)$ , and the phantom image  $x^* = (5, 6, 7, 2)^T$ ; and (ii) the image as the second example is made of 5 × 5 pixels and 56 projection rays with phantom image shown in Fig.1.

Figure 2 shows an ICC forming a torus observed in the map  $f$  for the first example ( $J = 4$ ) with  $\gamma = 2$ , consisting of 100,000 iterated points. The characteristic multipliers of the fixed point satisfy the condition of the double Neimark-Sacker bifurcation as a codimension two bifurcation.

Figure 3 shows a phase transition diagram of fixed points observed in the extended PMART of Eq.(9) with  $J = 4$ . In the figure, the parameter sets of equal values of characteristic multipliers of fixed points are indicated by solid and dashed curves with symbols  $\mu^* R$  and  $\rho^* C$ , in the case of real multiplier  $\mu^*$  and the absolute value  $\rho^*$  of complex multiplier, respectively, each of which is the maximum absolute value among all characteristic multipliers. Period-doubling and the Neimark-Sacker bifurcations are conventionally denoted by the symbols  $P$  and  $NS$ , which are equivalent to  $^{-1}R$  and  $^1C$ , respectively.

In the diagram, there exists a unique stable fixed point in the parameter regions without shading, and with shading patterns ,  and . Whereas, in the regions with patterns  and  surrounded by the Neimark-Sacker and period-doubling bifurcation curves, the fixed point is unstable and a solution does not converge to the fixed point corresponding to the phantom image. By increasing the value of  $\lambda$  for fixed, e.g.,  $\gamma = 0.9$ , through the bifurcation curve  $P$ ,

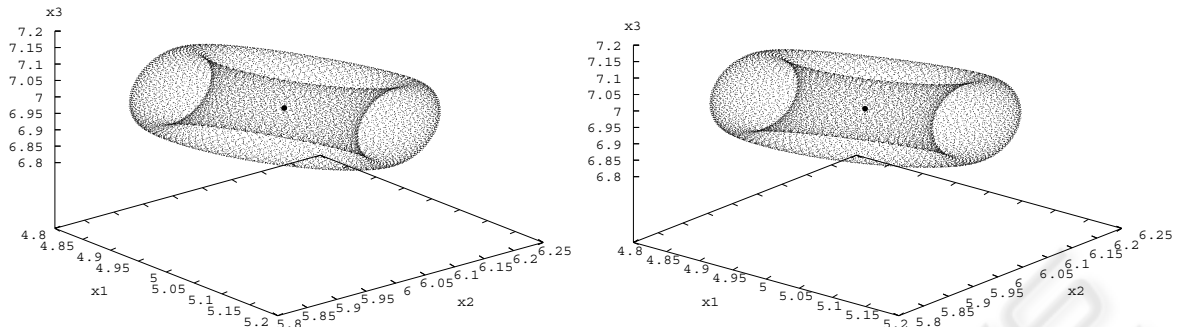


Figure 2: Perspective figure of an ICC observed in  $f$  with  $\gamma = 2$ . The fixed point is located at the circled point in the center of iterated points.

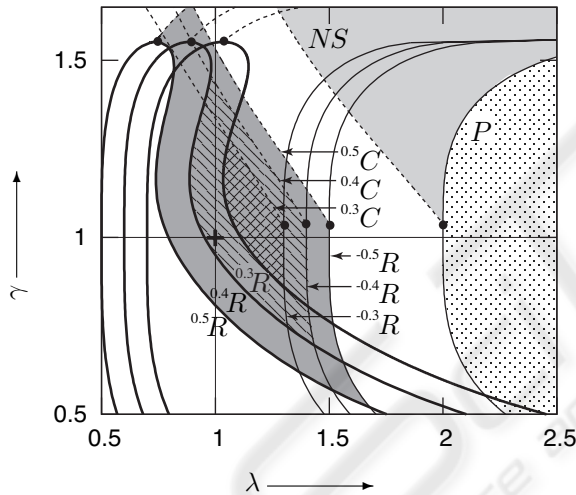


Figure 3: Phase transition of fixed points observed in  $g$  with  $J = 4$ .

the bifurcation formula is given by

$${}_0PD \rightarrow {}_1PI + {}_0PD^2$$

where the left- and right-hand sides of the arrow indicate invariant sets before and after the bifurcation, respectively. On the other hand, when the parameters pass through the Neimark-Sacker bifurcation curve  $NS$  in the direction from outside to inside the region  $\square$ , we have the following formula:

$${}_0PD \rightarrow {}_2PD + ICC$$

The parameter curves of equal characteristic multipliers are shown in the case of 0.3, 0.4 and 0.5 as their maximum absolute values. We see that there is a

fixed point with characteristic multipliers whose maximum absolute value is less than 0.3, in the region with pattern  $\square$ . Therefore, a parameter in this region gives a faster convergence in the neighborhood of the stable fixed point. Note that the system at the parameter  $(\lambda, \gamma) = (1, 1)$ , denoted by the symbol  $+$  in the diagram, corresponds to the MART, and the parameter point is located outside the region  $\square$ . Indeed, a simulation result compared with the extended PMART at  $(\lambda, \gamma) = (1.2, 1.05)$  and the MART is illustrated in Fig.4, showing the root mean square distance between the reconstructed value and the fixed point, normalized by the standard deviation (Gordon and Herman, 1974), for the time series. The initial state for the iterations was set to a constant image. In the figure, the lines (a) and (b) are results using the extended PMART and the MART, respectively. We see that the proposed method gives rise to faster convergence with a steep slope in log scale.

A phase transition for the second example ( $J = 25$ ) is shown in Fig.5. Similarly as the first example, we see that the parameter region  $\square$ , in which the maximum absolute of characteristic multiplier is minimum, does not include the parameter point  $(\lambda, \gamma) = (1, 1)$ .

## 5 CONCLUSION

We have investigated an extended PMART proposed in order to accelerate the convergence. For analyzing convergence speed in the neighborhood of the stable fixed point, we have proposed a computational method to calculate a set of equal value of characteristic multipliers, based on the dynamical system theory.

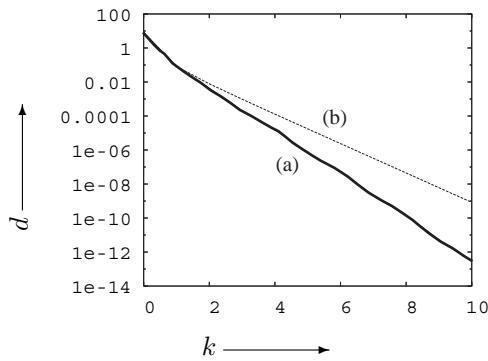


Figure 4: The distance  $d$  for the time series of (a) the extended PMART and (b) the MART.

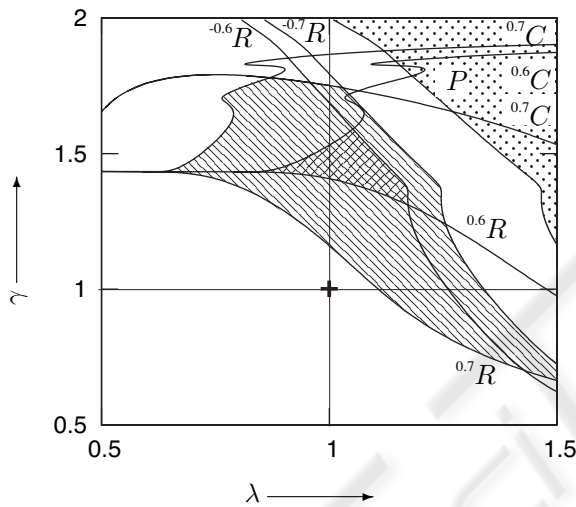


Figure 5: Phase transition of fixed points observed in  $g$  with  $J = 25$ .

Then, by numerical experiments of lower dimensional systems, we have obtained a parameter region which gives a faster convergence than the original MART. The performance of the acceleration depends on the dynamical property of the system with the parameters  $\gamma$  and  $\lambda$ . We should investigate the theoretical reason why the parameter region in which the maximum absolute value of characteristic multiplier is minimum, excludes the value  $(\lambda, \gamma) = (1, 1)$ .

## REFERENCES

Badea, C. and Gordon, R. (2004). Experiments with the nonlinear and chaotic behaviour of the multiplicative algebraic reconstruction technique (MART) algorithm for computed tomography. *Phys. Med. Biol.*, 49:1455–1474.

Byrne, C. (2004). A unified treatment of some iterative algorithms in signal processing and image reconstruction. *Inverse Problems*, 20:103–120.

Gordon, R., Bender, R., and Herman, G. (1970). Algebraic reconstruction technique (ART) for three-dimensional electron microscopy and x-ray photography. *J. Theoret. Biol.*, 29:471–482.

Gordon, R. and Herman, G. (1974). Three dimensional reconstruction from projections: a review of algorithms. *Int. Rev. Cytol.*, 38:111–151.

Herman, G. and Meyer, L. (1993). Algebraic reconstruction techniques can be made computationally efficient. *IEEE Trans. Med. Imag.*, 12(3):600–609.

Kak, A. and Slaney, M. (1987). *Principles of Computerized Tomographic Imaging*. Piscataway, NJ: IEEE Press.

Kawakami, H. (1984). Bifurcation of periodic responses in forced dynamic nonlinear circuits: computation of bifurcation values of the system parameters. *IEEE Trans. Circuits and Systems*, CAS-31(3):246–260.

Man, B., Nuyts, J., Dupont, P., Marchal, G., and Suetens, P. (2001). An iterative maximum-likelihood polychromatic algorithm for CT. *IEEE Trans. Med. Imag.*, 20(10):999–1008.

Mueller, K., Yagel, R., and Wheller, J. (1999). Anti-aliases three-dimensional cone-beam reconstruction of low-contrast objects with algebraic methods. *IEEE Trans. Med. Imag.*, 18(6):519–537.

Shepp, L. and Vardi, Y. (1982). Maximum likelihood reconstruction in positron emission tomography. *IEEE Trans. Med. Imag.*, 1:113–122.

Snyder, D., Schulz, T., and O’Sullivan, J. (1992). Deblurring subject to nonnegativity constraints. *IEEE Trans. Signal Processing*, 40(5):1143–1150.

Stark, H. (1987). *Image Recovery: Theory and Application*. FL: Academic.

Wang, G., Snyder, D., O’Sullivan, J., and Vannier, M. (1996). Iterative deblurring for CT metal artifact reduction. *IEEE Trans. Med. Imag.*, 15(5):657–664.